A Traceable Scatterometry Measurement of a Silicon Line Grating

Thomas A. Germer, Heather J. Patrick, and Ronald G. Dixson

Physical Measurements Laboratory, National Institute of Standards and Technology
100 Bureau Drive, Gaithersburg, Maryland 20899 USA

Abstract. In this paper, we present a spectroscopic Mueller matrix ellipsometry measurement of a silicon line grating with nominal pitch of 600 nm and line width 100 nm. An uncertainty analysis is performed on the measurement results. The results are compared to critical dimension atomic force microscopy (CD-AFM) measurements. Except for one of the gratings, the CD-AFM and scatterometry measurements lie within each other's uncertainties.

Keywords: Ellipsometry, Scatterometry, Silicon, Traceability
PACS: 06.20.fb, 06.30.Bp, 07.60.Fs, 42.25.Fx

INTRODUCTION

Scatterometry, sometimes referred to as optical critical dimension (OCD) metrology, combines reflectometry or ellipsometry with electromagnetic simulations to measure dimensions of features in periodic structures [1]. Optical scatterometry has become an attractive tool for dimensional metrology in the semiconductor industry, due in large part to its inline potential for providing critical feedback information necessary for tight process control. Unlike atomic force microscopy (AFM), which measures the dimensions of a target by physically contacting it, scatterometry measures those dimensions by obtaining an optical signature and comparing that signature to a theoretical parametric model. Until recently, however, little attention has been given to establishing absolute accuracy for optical scatterometry.

In this paper, we discuss the development of an independent uncertainty budget for an optical scatterometry measurement, an important step toward establishing traceability to the International System (SI) meter. One of the key developments has been a methodology for propagating systematic uncertainties and signal noise through a regression analysis [2]. The regression analysis optimizes a set of floating parameters [e.g., width, side wall angle (swa), and height] under a set of fixed assumptions (e.g., optical constants and instrument conditions). A scatterometry sensitivity analysis program, OCDSense, has been developed that implements this methodology for any grating structure and measurement scheme. OCDSense propagates the noise in the reflectance measurement and the uncertainties in the fixed parameters (assumptions) to the covariance matrix of the floating parameters. Uncertainties in incident angle, wavelength scale, numerical aperture, and spectral bandwidth, also contribute to the measurement uncertainty, and to some extent, these uncertainties can be included in OCDSense as well. Ultimately, an uncertainty budget for line profile needs to specify not just uncertainties in a single number (such as width or swa), but an uncertainty in the profile function. An uncertainty budget for a specific scatterometry measurement of a silicon trench grating will be presented.

SAMPLE AND MEASUREMENTS

Measurements were obtained from 100 µm × 100 µm scatterometry targets, produced using the SEMATECH Overlay Metrology Advisory Group 3 (OMAG3) reticule. The targets were silicon line gratings, etched into a silicon substrate. The wafer was produced using a focus exposure matrix such that targets on adjacent dies had fixed pitch but different linewidths. One target series was investigated having a pitch of 600 nm and a nominal width of 100 nm. There were nine such targets that were investigated in this study.

Measurements were performed using a Woollam M-1000 spectroscopic ellipsometer[1] with 11-element Mueller matrix and micro-focusing capability, spanning the wavelength range from 270 nm to 1000 nm and having a fixed, nominal incident angle of 65°. The instrument also has the capability to rotate the sample about its azimuth, enabling conical measurements. Data in this study were acquired for azimuth angles –90° (along the lines), –45°, 0° (along the grating direction), 45°, and 90° (also along the lines).

Analysis was carried out using software developed at NIST. The rigorous coupled wave (RCW) electromagnetic field solver is available online as part of the SCATMECH software library [3]. The non-linear least squares regression routine is based upon the Levenberg-Marquardt algorithm. The regression routine makes use of a high-performance clustered computing system by spreading the RCW simulations over many processors. Fits to the eleven normalized Mueller matrix elements were obtained using different combinations of azimuths in order to ensure the accuracy and stability of the profile model used. The weighting function was chosen to be uniform, so that the best fit minimizes the root-mean-square (rms) deviation between the measured data and the fit. The data sets were extremely large, so showing a comparison between the optical signature data and the best-fit model would be difficult. However, the rms deviations were about 0.02, the normalized Mueller matrix elements being in the interval [–1,1].

PROFILE MODEL

Analysis of scatterometry data requires a model for the profile of the grating under test. The model describes the profile parametrically and is used by the RCW field solver to simulate the optical signature. It is extremely important the profile model be accurate and physically plausible. For the grating described here, we use a profile shown schematically in Fig. 1. This profile model includes the presence of an oxide film and has an elliptical corner rounding at the bottom of the trenches. The corner rounding is approximated by a polygon with three segments. The profile was divided into 20 layers to be compatible with the RCW algorithm.

[1] Certain commercial equipment, instruments, or materials are identified in this paper in order to specify the experimental procedure adequately. Such identification is not intended to imply recommendation or endorsement by the National Institute of Standards and Technology, nor is it intended to imply that the materials or equipment identified are necessarily the best available for the purpose.

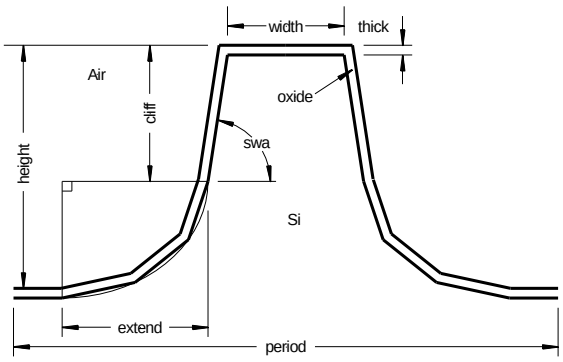

Figure 1. The profile model used to analyze the data and define the model parameters. This diagram is a schematic and is not to scale.

MEASUREMENT RESULTS

Table 1 outlines the measurement results for the target in the central (0,0) die. The values given represent all of the parameters that were varied in the measurement. The azimuth offset is the small angle that the grating is misaligned with the ellipsometer plane of incidence. It should be borne in mind that many of the parameters are specific to the model (such as extend and cliff), while others can be directly compared to other reference metrologies (such as height). We do not present the parameter variances or covariances between the parameters until later in the paper.

Table 1. Best fit parameters for the central (0,0) die.

Parameter	Value
width	111.4 nm
extend	33.2 nm
cliff	120.4 nm
height	229.9 nm
period	600.1 nm
oxide	1.9 nm
swa	87.12°
azimuth offset	–0.65°

UNCERTAINTY BUDGET

In this section we outline the various elements that contribute to uncertainty in the measurements. These are divided into three categories: the uncertainties that are associated with the reproducibility and repeatability of the measurement; those that are induced by the instrument; and those that are induced by the sample. The uncertainties are propagated using the formalism described in Ref. 2 and are carried out by the OCDSense program. Sensitivity of the optical signature to changes in each of the parameters is calculated numerically.

Noise (Type A)

Noise, or random fluctuations in the optical signature, contributes to the uncertainty in the profile. In our case, noise statistics for the instrument were determined in a previous study as a function of wavelength by performing a repeatability and reproducibility study with a variety of samples [4]. That study found a consistent noise spectrum and methodology for converting it to the optical signature. The instrument also reports noise statistics by estimating the standard deviation for each measured datum. These two assessments of the noise statistics agree within a factor of about two for most conditions. A third way to perform this analysis is to simply measure the optical signature several times and determine the spread in the resulting best fit parameters. For this study, the noise spectrum determined in the first study was used. In all of the cases, the uncertainties determined from noise in the optical signature are relatively small.

Instrument Contributions (Type B)

In this section we describe factors that contribute to uncertainties that arise from uncertainties in measurement parameters that are not fit during the parameter estimation. The length scale for scatterometry is related to the wavelength scale and the incident angles of the instrument. The relationship is not direct, in that, with the possible exception of the grating period, the dimensions cannot be simply determined from the wavelengths of features in the optical signature. However, through the simulation, these two factors ultimately provide the length scale of the measurement.

The incident angle, while being nominally 65°, was found to be 65.21° from a fit of data for an approximately 20 nm oxide film on silicon taken shortly before measurements were performed on the gratings. Measurements on an approximately 1 µm thick oxide on silicon would typically yield angles of incidence within about 0.5° of the value found from the 20 nm oxide. We thus let the standard uncertainty for the incident angle be 0.15° (assuming a uniform distribution of width 0.5°). Similarly, by fitting data for the thicker oxide to models with the numerical aperture, we estimate that the numerical aperture is 0.065 with an uncertainty of 0.003.

The wavelength scale of the instrument was determined in two different ways. One was to use Hg and Ar emission lines to calibrate the spectrometer [5]. The other was to use the thick oxide sample, in the same measurement that determined the numerical aperture and incident angles above. Both of these measurements yielded an offset from the factory-established scale of –0.3 nm. Assuming that the factory-established scale was a third calibration point, also performed with a Hg-Ar lamp, we assign an uncertainty of 0.2 nm to the wavelength scale (assuming a uniform distribution of width 0.6 nm). We also estimate the spectral bandwidth of the instrument to have a standard deviation of 1.5 nm, and estimate the uncertainty in that bandwidth to be 0.25 nm. The effects of the spectral bandwidth were not used in the fitting procedure, as it was found to have a very small effect in these measurements, and including these effects adds substantially to the fitting time.

Sample Contributions (Type B)

There are two main sources of error that can arise from the sample, namely the optical properties of the materials in the grating and that associated with the choice of profile model. The first was found by using two different tabulations of the optical constants and the extinction coefficients of silicon and silicon dioxide, each as a function of wavelength. In the case of the silicon dioxide, the values ranged from that reported for a thermal oxide to that reported for a native oxide. The curves for each of these were allowed to vary parametrically between each two available curves with a parameter x in the interval (0,1). The estimated uncertainties in the parameters x_{Si} (for silicon) and x_{oxide} (for silicon dioxide) were 0.3 (assuming a uniform distribution of width 1).

It is much more difficult to assess the uncertainty in the profile model, in large part because the model itself is not a single value, but rather a parameterization of the profile, and a simplification at that. In another study, we suggested that an alternative profile be used, which has roughly double the number of parameters, and which includes parameters for sidewall bulge and corner rounding [2]. Such a study was not carried out for this grating. The grating profile used here is believed to be sufficiently smooth and to reflect most of the conceivable features of the profile.

EXPRESSING UNCERTAINTY

The expression of uncertainty for a profile measurement needs to express not only the uncertainties in each of the profile values, but also the correlations between them. A covariance matrix expresses these correlations, but not in a particularly transparent manner. We choose to express the uncertainty by showing an ensemble of profiles that corresponds to the total uncertainty covariance matrix.

That is, we generate normally-distributed random numbers that follow the covariance matrix and generate profiles from them. Figure 2 shows 100 profiles, whose parameters follow the covariance properties of the random, noise-induced uncertainties and all of the uncertainties, respectively. The widths of the lines thus illustrate the approximately 99% confidence interval of the profile.

We provide the uncertainty budget for the grating parameters for the central (0,0) die in Table 2. While the table does not show the covariances between the parameters, which are better viewed in Fig. 2, it does allow the reader to assess which uncertainties contribute the most to the overall uncertainty in the profile measurement. That is, one can see that the incident angle and the substrate material optical properties contribute the most to the total uncertainty.

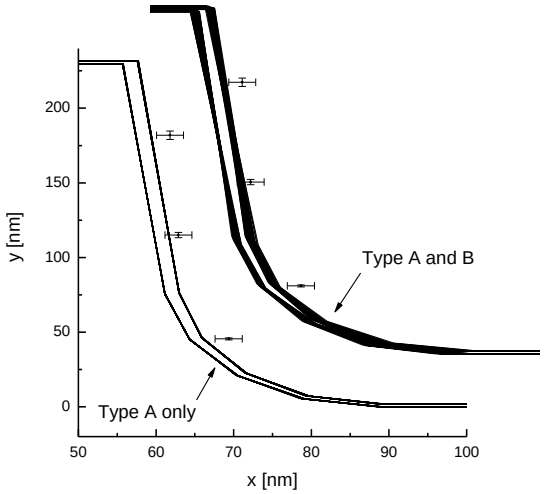

Figure 2. The best fit profile for the grating in the central die. Shown are 100 realizations of the profile with parameters consistent with the noise-induced (Type A) and total (Type A and B) covariance matrices. The vertical scale is different than the horizontal scale. Also shown are the results from the atomic force microscope measurements with expanded uncertainty (k=2) error bars.

COMPARISON WITH ATOMIC FORCE MICROSCOPY

Critical dimension atomic force microscopy (CD-AFM) measurements were performed on the samples. In these measurements, the height (h) and the widths of the lines at 0.2h, 0.5h, and 0.8h were measured. The uncertainties in the AFM measurements were 3.5 nm (k=2). These values are shown in Figure 2 for the central (0,0) die. For the center width (at 0.5h), the interval of the scatterometry results overlaps the interval of the AFM result. For the other two widths (at 0.2h and 0.8h), the scatterometry result underestimates the widths by a bit.

One of the lessons learned during this study is that when comparing measurements from different methods, the measurements must be compared on equal footing. Therefore, when we make the comparison, we determine the widths of our model grating at the same fractional heights as were measured with AFM. These values are given in Table 3 for each die, for both scatterometry and AFM. The agreement between the scatterometry results and the AFM results are overall very good. Most are well within the uncertainty of the AFM measurements. In fact, the central die (0,0), used for Fig. 2, has by far the largest discrepancy.

CONCLUSIONS

We performed spectroscopic ellipsometry measurements from a set of nine silicon line gratings and performed an uncertainty analysis of the results. For most of the results, the measurements agreed well with the AFM measurements. This study suggests that scatterometry measurements of simple gratings can be traceable to the SI without need for AFM reference metrology.

Table 2. Uncertainties in each of the fitting parameters (excluding rotation angle).

	width [nm]	extend [nm]	height [nm]	oxide [nm]	cliff [nm]	swa [°]	pitch [nm]
x_{oxide}	0.04	0.03	0.01	0.09	0.32	0.02	0.03
x_{Si}	0.15	0.36	0.19	0.06	0.42	0.15	0.08
Numerical aperture	0.02	0.10	0.01	0.00	0.23	0.02	0.01
Spectral bandwidth	0.03	0.04	0.05	0.00	0.25	0.00	0.15
Incident angle	0.59	1.27	0.39	0.03	2.70	0.40	0.17
Wavelength	0.03	0.18	0.10	0.02	0.68	0.03	0.36
Total, Type B	0.61	1.33	0.45	0.11	2.85	0.43	0.44
Noise, Type A	0.06	0.20	0.04	0.02	0.65	0.05	0.05
Total	0.61	1.35	0.45	0.11	2.92	0.43	0.44
Expanded uncertainty (k=2)	1.22	2.70	0.91	0.23	5.85	0.86	0.88

Table 3. Comparison between scatterometry and AFM measurements on the nine dies.

Die	Scatterometry				AFM				Differences			
	Widths [nm]			Height	Widths [nm]			Height	Widths [nm]			Height
	20 %	50 %	80 %	[nm]	20 %	50 %	80 %	[nm]	20 %	50 %	80 %	[nm]
(1,0)	131.0	122.1	117.5	229.9	135.3	120.3	122.3	227.8	–4.3	–0.2	–2.9	2.1
(1,1)	134.1	125.3	120.5	231.9	138.2	123.2	125.1	229.7	–4.1	0.2	–2.6	2.2
(0,1)	133.8	125.3	120.0	230.8	138.2	121.9	125.8	228.6	–4.4	–0.5	–1.8	2.2
(–1,1)	134.4	125.8	119.8	231.3	137.3	120.0	125.4	229.2	–2.9	0.4	–0.2	2.1
(0,0)	131.9	123.3	118.6	229.9	138.7	123.6	125.8	227.4	–6.8	–2.5	–5.0	2.5
(–1,0)	130.9	122.5	116.0	230.0	133.5	115.2	122.1	228.4	–2.5	0.4	0.8	1.6
(–1,–1)	124.6	116.3	107.8	230.4	127.6	107.3	117.1	228.7	–3.0	–0.8	0.5	1.7
(0,–1)	127.8	119.3	113.4	230.0	131.0	115.3	118.4	227.2	–3.2	0.9	–1.9	2.8
(1,–1)	127.3	118.8	113.1	229.7	129.1	113.4	116.5	227.6	–1.8	2.4	–0.2	2.0
								Average differences:	–3.7	0.0	–1.5	2.1
								Standard deviation of differences:	1.5	1.3	1.9	0.4

REFERENCES

1. Raymond, C.J., "Scatterometry for Semiconductor Metrology," in *Handbook of Silicon Semiconductor Metrology*, ed. Diebold, A.C., (Dekker, New York, 2001), pp. 477–514.
2. Germer, T.A., Patrick, H.J., Silver, R.M., and Bunday, B., "Developing an Uncertainty Analysis for Optical Scatterometry," in *Metrology, Inspection, and Process Control for Microlithography XXIII*, edited by Allgair, J.A., Proc. SPIE **7272**, 72720T (2009).
3. SCATMECH: Polarized Light Scattering C++ Class Library, available at http://pml.nist.gov/scatmech.
4. Report to International Sematech Manufacturing Initiative, December 2010.
5. Ralchenko, Y., Kramida, A.E., Reader, J., and NIST ASD Team (2010). *NIST Atomic Spectra Database* (ver. 4.0.1). National Institute of Standards and Technology, Gaithersburg, MD.